

# DELVING DEEPER: HIERARCHICAL VISUAL PERCEPTION FOR ROBUST VIDEO-TEXT RETRIEVAL

Zequn Xie<sup>\*†</sup>

Boyun Zhang<sup>\*†</sup>

Yuxiao Lin<sup>†</sup>

Tao Jin<sup>†</sup>

\* These authors contributed equally to this work.

† Zhejiang University

The corresponding author is Tao Jin.

## ABSTRACT

Video-text retrieval (VTR) aims to locate relevant videos using natural language queries. Current methods, often based on pre-trained models like CLIP, are hindered by video’s inherent redundancy and their reliance on coarse, final-layer features, limiting matching accuracy. To address this, we introduce the **HVP-Net (Hierarchical Visual Perception Network)**, a framework that mines richer video semantics by extracting and refining features from multiple intermediate layers of a vision encoder. Our approach progressively distills salient visual concepts from raw patch-tokens at different semantic levels, mitigating redundancy while preserving crucial details for alignment. This results in a more robust video representation, leading to new state-of-the-art performance on challenging benchmarks including MSRVTT, DiDeMo, and ActivityNet. Our work validates the effectiveness of exploiting hierarchical features for advancing video-text retrieval. Our codes are available at <https://github.com/boyun-zhang/HVP-Net>.

**Index Terms**— Video-Text Retrieval, Vision Transformer, Cross-modal Alignment, Video Representation Learning, Computer Vision

## 1. INTRODUCTION

Cross-modal retrieval aims to bridge the inherent heterogeneity gap between different data modalities by projecting them into a common latent space for similarity measurement [1, 2]. This paradigm and advanced feature fusion techniques have been successfully applied across various domains, including text-based person retrieval [3, 4], financial risk analysis [5, 6], fake news detection [7, 8], and sequential recommendation [9, 10]. In Video-Text Retrieval (VTR), this is often achieved by leveraging large pre-trained models like CLIP [11] to learn a joint video-text embedding space. However, a critical limitation persists: these approaches, even those employing more advanced multi-grained matching strategies [12, 13, 14], predominantly rely on features from the *final layer* of the vision encoder [15, 16, 17]. This practice leads to significant information redundancy by indiscriminately encoding all visual

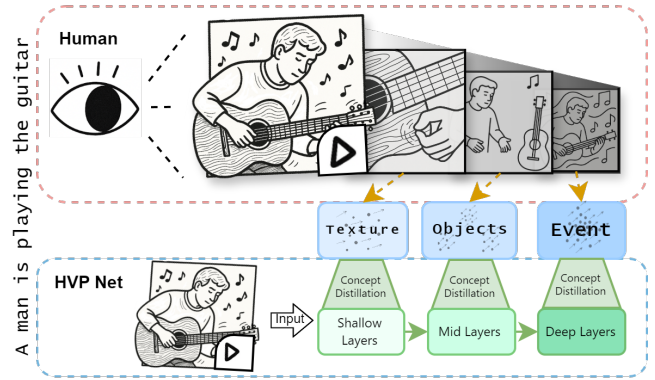


**Fig. 1.** Conceptual illustration of our HVP-Net, inspired by the human hierarchical perception process. Our model mimics this by processing visual data through shallow, mid, and deep layers to extract concepts ranging from low-level textures to high-level events.

tokens. More importantly, it overlooks the rich, hierarchical semantics and dynamics encapsulated within the encoder’s intermediate layers [18], thereby constraining both representation efficiency and matching precision.

## 2. METHODOLOGY

In this section, we detail our proposed **Hierarchical Visual Perception Network (HVP-Net)**. As illustrated in Figure 2, our core idea is to construct a robust video representation by extracting and refining features from multiple intermediate layers of a pre-trained vision encoder. The process involves three main stages: hierarchical feature encoding, a novel patch processing module, and multi-granularity alignment optimized via contrastive learning.

### 2.1. Hierarchical Feature Encoding

We use the pre-trained CLIP model [11] as our backbone. From its text encoder, we extract global sentence features

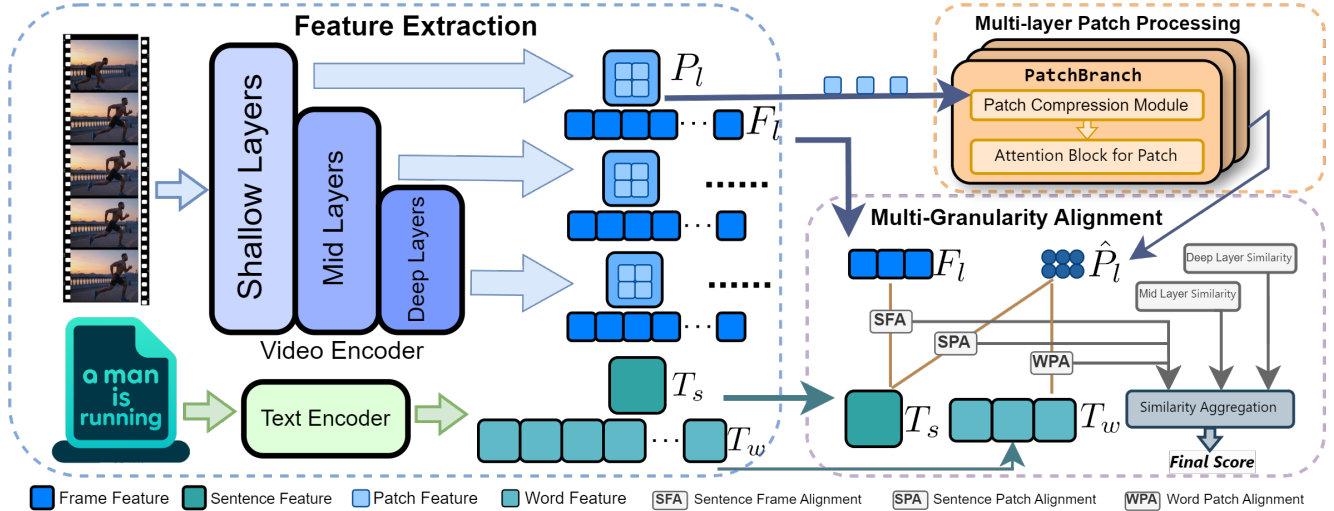


**Fig. 2.** The architecture of our HVP-Net. We first extract hierarchical frame ( $F_l$ ) and patch ( $P_l$ ) features from a video encoder. Then, our Multi-layer Patch Processing module refines the patch features into  $\hat{P}_l$ . Finally, we perform multi-granularity alignment between text and the multi-level video features ( $F_l, \hat{P}_l$ ) and aggregate the layer-wise similarity scores for retrieval.

$$T_s \in \mathbb{R}^D \text{ and word-level features } T_w \in \mathbb{R}^{L_w \times D}.$$

Distinct from prior work that relies on final-layer outputs, we extract features from a set of intermediate layers  $\mathcal{L}$  of the Vision Transformer. For a video with  $N$  frames, this provides hierarchical features for each layer  $l \in \mathcal{L}$ : frame features  $F_l \in \mathbb{R}^{N \times D}$  (from [CLS] tokens) and patch features  $P_l \in \mathbb{R}^{N \times M \times D}$  (from patch tokens, with  $M$  patches per frame). This coarse-to-fine representation is then fed into our refinement module.

## 2.2. Multi-layer Patch Processing (MPP)

To distill semantic concepts from redundant patch features, we introduce the **Multi-layer Patch Processing (MPP)** module, which iteratively refines patch features  $P_l$  from each layer  $l$ . Each iteration involves a "compression-refinement" cycle:

- Patch Compression Module** We first compute a saliency score for all  $M$  patch tokens. A Density-Peak Clustering (DPC) algorithm then dynamically identifies  $K$  cluster centers ( $K \ll M$ ) from these tokens. Finally, tokens are merged into  $K$  features via a saliency-weighted average based on cluster assignments.
- Attention Block for Patch:** The  $K$  compressed features act as queries in-a-cross-attention block, attending to the original  $M$  tokens to enrich the compressed representations with fine-grained details.

This iterative process outputs a purified patch feature set  $\hat{P}_l \in \mathbb{R}^{N \times K \times D}$  for each layer, forming a distilled multi-level representation of visual entities.

## 2.3. Multi-granularity Alignment and Optimization

To ensure precise retrieval, we perform cross-modal alignment across three semantic granularities, spanning all  $L$  extracted feature levels. For a given text-video pair  $(i, j)$ , we compute the following similarity scores for each layer  $l$ :

- Sentence-Frame (SF) Alignment:** Similarity between the global sentence feature  $T_{s_i}$  and the frame features  $F_{l_j}$ .
- Sentence-Patch (SP) Alignment:** Similarity between  $T_{s_i}$  and the refined patch concepts  $\hat{P}_{l_j}$ .
- Word-Patch (WP) Alignment:** Similarity between word features  $T_{w_i}$  and refined patch concepts  $\hat{P}_{l_j}$ .

For patch-level and word-level features, the final similarity score is not derived from simple pooling. Instead, we first identify the most relevant patch for each word token (and vice versa) using max-pooling over the token-to-patch similarity matrix. Then, we employ learnable weights, predicted by small MLPs, to perform a weighted aggregation of these maximum similarity scores. This allows the model to dynamically emphasize the most salient word and patch contributions. For a given layer  $l$ , the word-to-patch similarity component is calculated as:

$$S_{w \rightarrow p}^{(l)}(i, j) = \sum_{k=1}^{N_w} W_{\text{MLP}}(w_{ik}) \cdot \max_{m=1}^{N_p} \text{sim}(w_{ik}, p_{jm}) \quad (1)$$

A symmetric patch-to-word similarity is also computed, and the final score is their average.

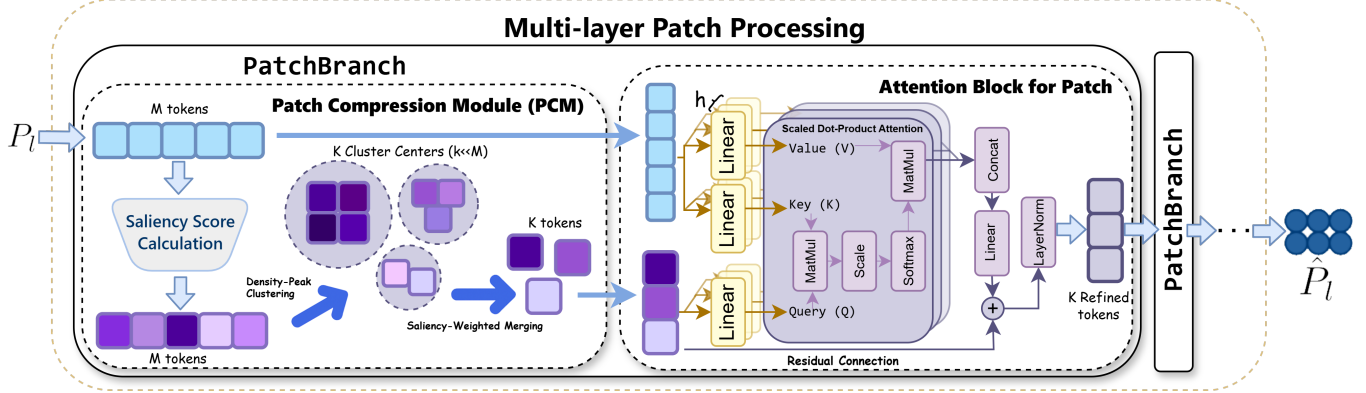


**Fig. 3.** The architecture of the Multi-layer Patch Processing (MPP) module, which iteratively refines input patch features  $P_l$  to  $\hat{P}_l$ . In each processing block, a Patch Compression Module (PCM) first distills  $M$  tokens into  $K$  core concepts using saliency-guided clustering. Subsequently, these concepts are refined via a cross-attention mechanism that attends back to the original tokens.

**Objective Function.** We optimize the model using a symmetric contrastive loss (InfoNCE) [19]. The total loss is the sum of bidirectional contrastive losses computed for each alignment granularity at each feature level:

$$\mathcal{L}_{\text{total}} = \sum_{l=1}^L (\mathcal{L}_{\text{SF}}^{(l)} + \mathcal{L}_{\text{SP}}^{(l)} + \mathcal{L}_{\text{WP}}^{(l)}) \quad (2)$$

where each component, e.g.,  $\mathcal{L}_{\text{SF}}^{(l)}$ , is a standard InfoNCE loss calculated on the sentence-frame similarity matrix for layer  $l$ . This joint optimization across multiple levels and granularities ensures the learning of a consistent and robust cross-modal semantic space.

**Inference.** At inference time, the final similarity score between a query text and a candidate video is the sum of all similarity scores computed across all granularities and layers, maintaining consistency with the training objective.

### 3. EXPERIMENTS

We conduct extensive experiments to evaluate our proposed HVP-Net. We first introduce the experimental setup, then compare our method with state-of-the-art (SOTA) approaches, and finally provide in-depth analysis through ablation studies and qualitative examples.

#### 3.1. Experimental Setup

**Datasets and Metrics.** Our evaluation is performed on three mainstream benchmarks: **MSR-VTT** [20], **DiDeMo** [21], **ActivityNet Captions** [22]. For MSR-VTT, we follow the standard ‘1k-A’ test split. We use standard retrieval metrics: **Recall at K (R@K, K=1, 5, 10)** (higher is better), **Median Rank (MdR)**, and **Mean Rank (MnR)** (lower is better), for both text-to-video (T2V) and video-to-text (V2T) tasks.

**Implementation Details.** Our model is built upon the CLIP ViT-B/32 backbone. We uniformly sample 12 frames per video at 224x224 resolution, with a maximum text length of 24 tokens. We use an initial learning rate of 1e-4 (a coefficient of 0.001 for the CLIP backbone) and a weight decay of 0.2. The model is trained for 5 epochs on MSR-VTT with a batch size of 32. The MPP module processes features extracted from three layers of the vision encoder: a shallow (1st), a middle (6th), and a deep (12th) Transformer layer.

#### 3.2. Comparison with State-of-the-Art Methods

We compare HVP-Net against recent SOTA methods, including strong CLIP-based models like CLIP4Clip [15], X-CLIP [17], BiHSSP[23], MUSE[24].

**Table 1.** Performance comparison on the MSR-VTT 1k-A test set. R@K is in percentage (%). Best results are in **bold**.

Method	R@1↑	R@5↑	R@10↑	MdR↓	MnR↓
<i>Text-to-Video (T2V)</i>					
CLIP4Clip [15]	44.5	71.4	81.6	2.0	15.3
X-CLIP [17]	49.3	75.8	84.8	2.0	12.2
BiHSSP[23]	48.1	74.0	84.1	2.0	12.1
MUSE[24]	50.9	76.7	85.6	1.0	10.9
<b>HVP-Net (ours)</b>	<b>56.7</b>	<b>83.9</b>	<b>90.6</b>	<b>1.0</b>	<b>5.3</b>
<i>Video-to-Text (V2T)</i>					
CLIP4Clip [15]	42.7	70.9	80.6	2.0	11.6
X-CLIP [17]	48.9	76.8	84.5	2.0	8.1
BiHSSP[23]	48.0	74.1	83.5	2.0	9.0
MUSE[24]	49.7	77.8	86.5	2.0	7.4
<b>HVP-Net (ours)</b>	<b>50.5</b>	<b>80.5</b>	<b>91.2</b>	<b>2.0</b>	<b>4.4</b>

As shown in Table 1, HVP-Net significantly surpasses all competitors on MSR-VTT. For text-to-video retrieval, our method achieves an R@1 of 56.7%, outperforming the strongest baseline MUSE by a substantial 5.8% margin. This leading performance is consistent across all metrics for both

text-to-video and video-to-text tasks. Table 2 further confirms our model’s superiority and generalization, as it establishes new state-of-the-art results on both DiDeMo and ActivityNet, outperforming prior works across all reported recall metrics.

**Table 2.** Performance comparison with state-of-the-art methods on DiDeMo and ActivityNet for text-to-video retrieval.

Method	DiDeMo			ActivityNet		
	R@1↑	R@5↑	R@10↑	R@1↑	R@5↑	R@10↑
Clip4Clip [15]	-	-	-	40.5	72.4	83.6
CLIP-VIP [25]	48.6	77.1	84.4	-	-	-
HBI [26]	-	-	-	42.2	73.0	84.6
DiffusionRet [27]	46.7	74.7	82.7	-	-	-
<b>HVP-Net (Ours)</b>	<b>57.1</b>	<b>83.1</b>	<b>87.0</b>	<b>43.5</b>	<b>78.3</b>	<b>88.2</b>

### 3.3. Ablation Studies and Analysis

We conduct comprehensive ablation studies on the MSR-VTT dataset to analyze the key components of HVP-Net. All results for the T2V task are reported in Table 3.

**Effectiveness of Core Components.** We first validate our two main contributions: the multi-layer strategy and the Multi-layer Patch Processing module. As shown in Table 3 (left), a baseline using only final-layer features achieves an R@1 of 54.2%. The full HVP-Net model boosts performance to 56.7%. Notably, simply aggregating raw intermediate features without our proposed MPP module (+ Multi-layer (w/o MPP)) leads to a dramatic performance collapse (22.1%), confirming that our purification process is essential for effectively fusing multi-layer information.

**Impact of Layer Selection.** We analyze different layer selection strategies in Table 3 (middle). While using contiguous Last 3 layers (55.6%) improves over the Last 1 layer baseline (54.2%), our default strategy of sampling from diverse semantic stages (1, 6, 12) performs best (56.7%). This supports our hypothesis that fusing low-level details with high-level semantics is beneficial. Using more layers (1, 3, 6, 9, 12) degrades performance (51.9%), indicating our three-stage sampling is an efficient and effective choice.

**Impact of Alignment Losses.** Finally, ablating each loss component (Table 3, right) confirms their necessity. Removing the sentence-frame ( $\mathcal{L}_{SF}$ ), sentence-patch ( $\mathcal{L}_{SP}$ ), or word-patch ( $\mathcal{L}_{WP}$ ) alignment losses leads to performance drops of **8.5**, **3.5**, and a substantial **23.4** points, respectively. This demonstrates that all three supervision levels are crucial, with the fine-grained word-patch alignment being the most impactful component for robust cross-modal understanding.

## 4. CONCLUSION

In this paper, we addressed the critical challenge of information redundancy in text-video retrieval, a limitation of con-

**Table 3.** Ablation studies on core components, layer selection strategy, and loss functions (T2V R@1, %).  $\Delta$  denotes the performance drop from the full model.

Component Ablation	R@1	Layer Selection	R@1	Loss Ablation	R@1 ( $\Delta$ )
Baseline (Last 1 layer)	54.2	Last 1 layer	54.2	Full Model	56.7 (-)
+ Multi-layer (w/o MPP)	22.1	Last 3 layers	55.6	w/o $\mathcal{L}_{SF}$	48.2 (-8.5)
+ MPP (Full Model)	<b>56.7</b>	5 layers 1,3,6,9,12	51.9	w/o $\mathcal{L}_{SP}$	53.2 (-3.5)
		<b>Default 1,6,12</b>	<b>56.7</b>	w/o $\mathcal{L}_{WP}$	33.3 (-23.4)

ventional methods that rely solely on final-layer features. We proposed the **HVP-Net**, a novel framework featuring a **Multi-layer Patch Processing (MPP) Module**. This module effectively distills salient concepts by refining features from the intermediate layers of a vision encoder, creating a more robust cross-modal embedding space. Our approach establishes new state-of-the-art performance on multiple benchmarks, including a notable R@1 of 56.7% on MSR-VTT. Our work validates that mining the internal hierarchical features of pre-trained models is a potent strategy for cross-modal alignment. Future work could explore adaptive layer-selection strategies and specific mechanisms to improve video-to-text retrieval performance.

## 5. REFERENCES

- [1] Zhichao Han, Azreen Bin Azman, Mas Rina Binti Mustaffa, and Fatimah Binti Khalid, “Cross-modal retrieval: A review of methodologies, datasets, and future perspectives,” *IEEE Access*, vol. 12, pp. 115716–115741, 2024.
- [2] Fang Feng, Xiaofei Wang, and Rushi Li, “Cross-modal retrieval with correspondence autoencoder,” in *Proceedings of the 22nd ACM international conference on Multimedia*, 2014, pp. 7–16.
- [3] Zequn Xie, Haoming Ji, Chengxuan Li, and Lingwei Meng, “Dynamic uncertainty learning with noisy correspondence for text-based person search,” 2025.
- [4] Zequn Xie, Chuxin Wang, Yeqiang Wang, Sihang Cai, Shulei Wang, and Tao Jin, “Chat-driven text generation and interaction for person retrieval,” in *Proceedings of the 2025 Conference on Empirical Methods in Natural Language Processing*, 2025, pp. 5259–5270.
- [5] Zong Ke, Yuqing Cao, Zhenrui Chen, Yuchen Yin, Shouchao He, and Yu Cheng, “Early warning of cryptocurrency reversal risks via multi-source data,” *Finance Research Letters*, p. 107890, 2025.
- [6] Zong Ke, Jiaqing Shen, Xuanyi Zhao, Xinghao Fu, Yang Wang, Zichao Li, Lingjie Liu, and Huailing Mu, “A stable technical feature with gru-cnn-ga fusion,” *Applied Soft Computing*, p. 114302, 2025.

[7] Weihai Lu, Yu Tong, and Zhiqiu Ye, “Dammfnd: Domain-aware multimodal multi-view fake news detection,” in *Proceedings of the AAAI Conference on Artificial Intelligence*, 2025, vol. 39, pp. 559–567.

[8] Yu Tong, Weihai Lu, Xiaoxi Cui, Yifan Mao, and Zhe-jun Zhao, “Dapt: Domain-aware prompt-tuning for multimodal fake news detection,” in *Proceedings of the 33rd ACM International Conference on Multimedia*, 2025, pp. 7902–7911.

[9] Weihai Lu and Li Yin, “Dmmd4sr: Diffusion model-based multi-level multimodal denoising for sequential recommendation,” in *Proceedings of the 33rd ACM International Conference on Multimedia*, 2025, pp. 6363–6372.

[10] Xiaoxi Cui, Weihai Lu, Yu Tong, Yiheng Li, and Zhejun Zhao, “Multi-modal multi-behavior sequential recommendation with conditional diffusion-based feature denoising,” in *Proceedings of the 48th International ACM SIGIR Conference on Research and Development in Information Retrieval*, 2025, pp. 1593–1602.

[11] Alec Radford, Jong Wook Kim, Chris Hallacy, Aditya Ramesh, Gabriel Goh, Sandhini Agarwal, Girish Sastry, Amanda Askell, Pamela Mishkin, Jack Clark, Gretchen Krueger, and Ilya Sutskever, “Learning transferable visual models from natural language supervision,” 2021.

[12] Xiaohan Wang, Linchao Zhu, and Yi Yang, “T2vlad: Global-local sequence alignment for text-video retrieval,” 2021.

[13] Shaobo Min, Weijie Kong, Rong-Cheng Tu, Dihong Gong, Chengfei Cai, Wenzhe Zhao, Chenyang Liu, Sixiao Zheng, Hongfa Wang, Zhifeng Li, and Wei Liu, “Hunyuan\_tvr for text-video retrieval,” 2022.

[14] Lisai Zhang, Hong Wu, Qing Chen, Yuan Deng, Jochen Siebert, Zili Li, Yuhan Han, Dong Kong, and Zhe Cao, “Vldeformer: Vision–language decomposed transformer for fast cross-modal retrieval,” *Knowledge-Based Systems*, vol. 252, pp. 109316, 2022.

[15] Huaishao Luo, Lei Ji, Ming Zhong, Yang Chen, Wen Lei, Nan Duan, and Tianrui Li, “Clip4clip: An empirical study of clip for end to end video clip retrieval,” 2021.

[16] Xun Yang, Jianfeng Dong, Yixin Cao, Xun Wang, Meng Wang, and Tat-Seng Chua, “Tree-augmented cross-modal encoding for complex-query video retrieval,” 2020.

[17] Yiwei Ma, Guohai Xu, Xiaoshuai Sun, Ming Yan, Ji Zhang, and Rongrong Ji, “X-clip: End-to-end multi-grained contrastive learning for video-text retrieval,” 2022.

[18] Yao Lu, Wen Yang, Yunzhe Zhang, Zuohui Chen, Jinyin Chen, Qi Xuan, Zhen Wang, and Xiaoniu Yang, “Understanding the dynamics of dnns using graph modularity,” in *European Conference on Computer Vision*. Springer, 2022, pp. 225–242.

[19] Aäron van den Oord, Yazhe Li, and Oriol Vinyals, “Representation learning with contrastive predictive coding,” *ArXiv*, vol. abs/1807.03748, 2018.

[20] Jun Xu, Tao Mei, Ting Yao, and Yong Rui, “Msr-vtt: A large video description dataset for bridging video and language,” in *2016 IEEE Conference on Computer Vision and Pattern Recognition (CVPR)*, 2016, pp. 5288–5296.

[21] Lisa Anne Hendricks, Oliver Wang, Eli Shechtman, Josef Sivic, Trevor Darrell, and Bryan Russell, “Localizing moments in video with natural language,” 2017.

[22] Ranjay Krishna, Kenji Hata, Frederic Ren, Li Fei-Fei, and Juan Carlos Niebles, “Dense-captioning events in videos,” in *2017 IEEE International Conference on Computer Vision (ICCV)*, 2017, pp. 706–715.

[23] Yang Liu, Shudong Huang, Deng Xiong, and Jiancheng Lv, “Learning dynamic similarity by bidirectional hierarchical sliding semantic probe for efficient text video retrieval,” *Proceedings of the AAAI Conference on Artificial Intelligence*, vol. 39, no. 6, pp. 5667–5675, Apr. 2025.

[24] Haoran Tang, Meng Cao, Jinfa Huang, Ruyang Liu, Peng Jin, Ge Li, and Xiaodan Liang, “Muse: Mamba is efficient multi-scale learner for text-video retrieval,” 2025.

[25] Hong Xue, Yuchong Sun, Bei Liu, Jianlong Fu, Rui Song, Houqiang Li, and Jiebo Luo, “Clip-vip: Adapting pre-trained image-text model to video-language alignment,” in *The Eleventh International Conference on Learning Representations*, 2022.

[26] Peng Jin, Jin Huang, Peng Xiong, Shizhe Tian, Chang Liu, Xiang Ji, Li Yuan, and Jian Chen, “Video-text as game players: Hierarchical banzhang interaction for cross-modal representation learning,” in *Proceedings of the IEEE/CVF Conference on Computer Vision and Pattern Recognition*, 2023, pp. 2472–2482.

[27] Peng Jin, Hao Li, Zekai Cheng, Ke Li, Xiang Ji, Chang Liu, Li Yuan, and Jian Chen, “Diffusionret: Generative text-video retrieval with diffusion model,” in *Proceedings of the IEEE/CVF international conference on computer vision*, 2023, pp. 2470–2481.